Field-dependent anisotropic magnetic coupling in layered ferromagnetic $Fe_{3-x}GeTe_2$

Wei Liu,[1,2] Yamei Wang,[1,2] Jiyu Fan,[3] Li Pi,[1,4] Min Ge,[4] Lei Zhang ⓘ,[1,*] and Yuheng Zhang[1,4]

[1]*Anhui Key Laboratory of Condensed Matter Physics at Extreme Conditions, High Magnetic Field Laboratory,*
Chinese Academy of Sciences, Hefei 230031, China
[2]*University of Science and Technology of China, Hefei 230026, China*
[3]*Department of Applied Physics, Nanjing University of Aeronautics and Astronautics, Nanjing 210016, China*
[4]*Hefei National Laboratory for Physical Sciences at the Microscale, University of Science and Technology of China, Hefei 230026, China*

Two-dimensional layered itinerant ferromagnetic $Fe_{3-x}GeTe_2$ is considered as a candidate for applications in heterostructure-based spintronics because of its near-room-temperature Curie temperature and highly tunable characteristic of ferromagnetism. Moreover, the strong anisotropic magnetism of $Fe_{3-x}GeTe_2$ is another great advantage for fabricating magnetic storage devices. However, many relevant properties of its anisotropy still remain poorly understood, especially the basic mechanism of anisotropic magnetic interaction. In this work, we focus on the study of magnetic coupling in single-crystal $Fe_{3-x}GeTe_2$ ($x \approx 0.28$) by the anisotropic magnetization, magnetic entropy change, and critical behavior. Our results confirm that the magnetization is angle dependent [$M(\varphi)$], in which the easy magnetic axis is along the c axis while it exhibits absolute isotropic property in the ab plane. The magnetic entropy change [ΔS_M] also reveals an anisotropic feature between $H//c$ and $H//ab$. By fitting the field-dependent parameters of $\Delta S_M(T, H)$, it gives the critical exponents $\beta = 0.361(3)$, $\gamma = 1.736(7)$, and $\delta = 5.806(8)$ for $H//c$, while $\beta = 0.714(3)$, $\gamma = 1.243(7)$, and $\delta = 2.741(1)$ for $H//ab$. The critical exponents with $H//c$ belong to the theoretical prediction of three-dimensional Heisenberg model, which suggest a short-range magnetic coupling. However, the critical exponents with $H//ab$ are close to those of mean-field model, which indicates a long-range magnetic coupling. The determined critical exponents suggest that the anisotropic magnetic coupling of $Fe_{3-x}GeTe_2$ is strongly dependent on orientations of the applied magnetic field.

I. INTRODUCTION

Two-dimensional (2D) van der Waals (vdW) bonded systems have gained a great deal of attention because of their highly tunable physical properties and immense potential applications [1–4]. In particular, 2D vdW bonded ferromagnets, such as $Cr_2Ge_2Te_6$, CrI_3, and Fe_3GeTe_2, have been investigated extensively owing to their excellent properties in magnetic, magnetoelectric, and magneto-optic areas [5–8]. The exploration of intrinsic ferromagnetism in 2D systems is extremely significant both for uncovering the fundamental low-dimensional magnetism and for developing the next-generation nanoscale spintronic devices [7–9]. These layered materials can be easily exfoliated down to a few layers or even a monolayer, which can retain ferromagnetic order at finite temperatures. Exotic layered-number-dependent properties are usually revealed in these systems [4–6].

The layered $Fe_{3-x}GeTe_2$ is an itinerant ferromagnet composed of 2D layers weakly connected by vdW bonding, which exhibits exotic physical phenomena such as nontrivial anomalous Hall effect [10–13], Kondo lattice behavior [14], strong electron correlations [15], and unusual magnetic domain structures [16,17]. The cell of $Fe_{3-x}GeTe_2$ displays a hexagonal structure belonging to space group $P6_3/mmc$,

where the 2D layers of $Fe_{3-x}Ge$ sandwiched between nets of Te ions are weakly connected by vdW bonding [18]. There are two inequivalent Fe atomic sites in $Fe_{3-x}GeTe_2$, which are denoted as Fe1 and Fe2. Fe1-Fe1 dumbbells are located at the center of every hexagonal cell in the honeycomb lattice, composed of covalently bonded Fe2-Ge atoms [10]. Among the reported 2D ferromagnetic materials, the high Curie temperature $T_C \sim 230$ K in bulk is the most prominent feature for $Fe_{3-x}GeTe_2$ [18]. Meanwhile, its T_C is dependent on the concentration of Fe atoms, ranging from 140 to 230 K with the variation of Fe concentration [19]. More important, T_C of $Fe_{3-x}GeTe_2$ is also dependent on the numbers of layers, which can be raised up to room temperature by the ionic gate method [6]. Because of the raising of T_C to room temperature and gate tunability, $Fe_{3-x}GeTe_2$ offers a platform to study the electronically controlled magnetism [3,6]. It is also a good candidate for heterostructure-based applications in spin-based quantum information technology [20,21].

Except for its high Curie temperature, layered $Fe_{3-x}GeTe_2$ possesses a large magnetic anisotropy energy, which is required for practical application in storage [15,22,23]. Since the easy axis of magnetization is along the c axis, most studies are concentrated on the properties with $H//c$. However, $Fe_{3-x}GeTe_2$ actually exhibits very different behaviors depending on orientations of the applied field [11,24,25]. Moreover, the detailed anisotropic properties involving $H//ab$ have not been adequately studied. In this work, we make systematic

---
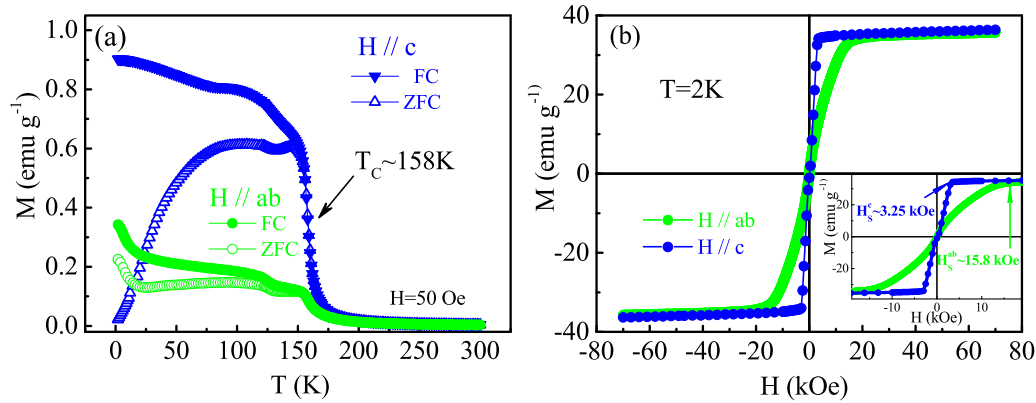
*Corresponding author: zhanglei@hmfl.ac.cn

FIG. 1. (a) Temperature dependence of magnetization [$M(T)$] for Fe$_{3-x}$GeTe$_2$ with $H//ab$ and $H//c$; (b) isothermal magnetization [$M(H)$] at $T = 2$ K with $H//ab$ and $H//c$ [inset shows magnified $M(H)$ in the low-field region].

investigations on the anisotropic behaviors of Fe$_{3-x}$GeTe$_2$ by the anisotropic magnetization, magnetic entropy change, and critical behaviors. The angle-dependent magnetism displays strong magnetization along the c axis, while it exhibits absolute isotropic characteristic in the ab plane. The anisotropic magnetic entropy changes give two series of critical exponents for $H//c$ and $H//ab$, which suggest strong field-dependent magnetic coupling in Fe$_{3-x}$GeTe$_2$.

II. EXPERIMENTAL METHODS

Single-crystal Fe$_{3-x}$GeTe$_2$ was synthesized by the self-flux technique [19]. The crystal structure of Fe$_{3-x}$GeTe$_2$ was checked by x-ray diffraction (XRD), which was performed on a Rigaku-TTR3 x-ray diffractometer with high-intensity graphite monochromatized Cu Kα radiation. The chemical composition was carefully determined by energy dispersive x-ray (EDX) spectrometry, which gives that the vacancy of Fe is $x \sim 0.28$. The angle-, temperature-, and field-dependent magnetization measurements were carried out by a Quantum Design vibrating sample magnetometer (SQUID-VSM). In particular, the initial isothermal magnetization with field applied along the c axis and within the ab plane was measured to obtain the magnetic entropy change. Before each measurement, the sample was warmed to room temperature. After being held at that temperature for 2 min, the sample was cooled to the target temperature under zero field to get the initial magnetizing curves. The magnetic field and temperature were relaxed before data collection, and a no-overshoot mode was employed to ensure a precise magnetic field.

III. RESULTS AND DISCUSSION

Figure 1(a) shows the temperature dependence of magnetization [$M(T)$] for the single-crystal Fe$_{3-x}$GeTe$_2$ with the field applied within the ab plane ($H//ab$) and along the c axis ($H//c$), respectively. As temperature decreases, the single-crystal layered Fe$_{3-x}$GeTe$_2$ undergoes a paramagnetic-to-ferromagnetic (PM-FM) transition at $T_C \sim 158$ K with both $H//ab$ and $H//c$. It is known that T_C is affected by the vacancy of Fe. The flux-grown crystals typically have a lower $T_C \approx 150$ K due to the Fe vacancy [19]. It has been demonstrated that Fe vacancy occurs only in the Fe2 sites, whereas

no Fe atoms occupy the interlayer space so that it does not affect the vdW interactions between adjacent layers [26]. The $M(T)$ curves with different external field orientations exhibit very distinctive behaviors. The magnetization with $H//c$ is larger than that with $H//ab$, and the phase transition is more sharp. When $H//c$, a bifurcation occurs just below T_C between the zero field cooling (ZFC) and field cooling (FC) curves. The FC curve increases while the ZFC curve decreases as the temperature cools. The decrease of $M(T)$ in low temperature is suggested to source from the antiferromagnetic interaction [27]. When $H//ab$, a similar bifurcation also occurs between the ZFC and FC curves. However, the $M(T)$ curves exhibit a upward trend at low temperature when $H//ab$. The magnetic behaviors are in agreement with previous reports [19,28]. It is noticed that a weak kink appears at ≈ 120 K below T_C, which is manifested as two-stage magnetic ordering behavior in this system due to the antiferromagnetic interaction [12,27]. Figure 1(b) shows the field-dependent isothermal magnetization [$M(H)$] at $T = 2$ K with $H//ab$ and $H//c$. It can be seen that the easy magnetization axis is along the c axis. The saturation field with $H//c$ ($H_S^c \sim 3.25$ kOe) is far smaller than that with $H//ab$ ($H_S^{ab} \sim 15.8$ kOe).

In order to clarify the magnetization evolution between different directions, the 3D plot of angle-dependent magnetization [$M(\varphi)$] at $T = 2$ K is shown in Fig. 2. The xy plane of Fig. 2 gives the in-plane $M(\varphi)$ with the field rotated within the ab plane. All the in-plane $M(\varphi)$ curves display perfect circular shape regardless of the orientations of field, which suggests an isotropic magnetism in the ab plane. The xz plane of Fig. 2 shows the out-of-plane $M(\varphi)$ with the field rotated from the ab plane to the c axis. In the higher field exceeding H_S, the $M(\varphi)$ curve presents a perfectly circular shape. However, obvious anisotropic behaviors appear for curves under lower fields, as shown in the xz plane of Fig. 2. The magnetization exhibits the minimum when $H//ab$ and it reaches the maximum when $H//c$, which confirms that the easy axis of magnetization is along the c axis. The $M(\varphi)$ behaviors of Fe$_{3-x}$GeTe$_2$ are very analogous to those of Cr$_2$Ge$_2$Te$_6$, which is also a 2D-layered ferromagnetic material [29].

In view of the strong magnetic anisotropy in this system, the magnetic properties with both $H//ab$ and $H//c$ should be investigated. Figures 3(a) and 3(b) give the field dependence of initial isothermal magnetization [$IM(H)$] around T_C with
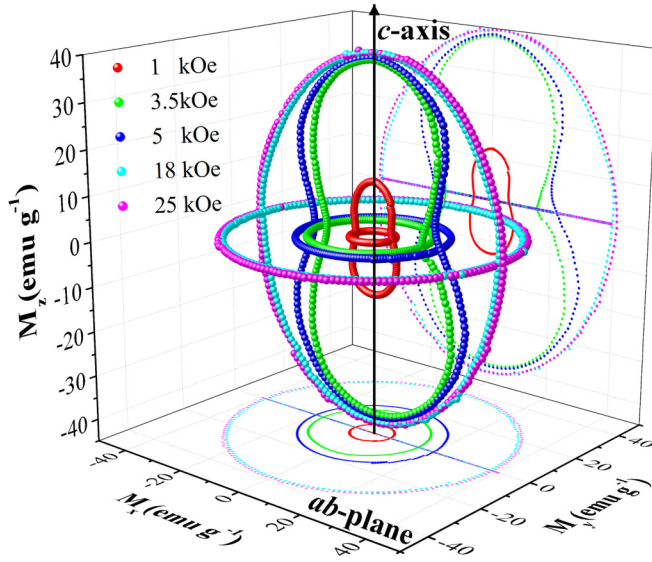
FIG. 2. The 3D plot of angle-dependent magnetization $[M(\varphi)]$ at $T = 2\,\mathrm{K}$ under the selected field: in plane $M(\varphi)$ (xy plane) with H rotated within the ab plane; out of plane $M(\varphi)$ (xz plane) with H rotated from the ab plane to the c axis.

$H//ab$ and $H//c$, respectively. It can be seen that $IM(H)$ curves with $H//ab$ and $H//c$ exhibit similar magnetic saturation behaviors. However, the magnetizing paths in lower field region are different. The magnetization with $H//c$ becomes saturated with a much sharper tendency than that with $H//ab$. In addition, the saturation magnetization (M_S) with $H//c$ is bigger than that with $H//ab$ at the same temperature.

As is known, the magnetic entropy change is correlated with the critical behavior of the phase transition. Actually, the parameters of magnetic entropy change are determined by the critical exponents, which can uncover the intrinsic physics such as type of the magnetic coupling, decay distance of spin interaction, spatial and spin dimensionality, long- or short-range magnetic interaction, etc. [30]. Thus, study of the magnetic entropy change and its parameters can deliver intrinsic mechanisms on the critical behavior of the phase transition. The magnetic entropy change with $H//ab$ and $H//c$ can be obtained based on the $IM(H)$ curves to investigate the anisotropic magnetic interactions. The magnetic

entropy change $[\Delta S_M(T, H)]$ induced by the external field is calculated as [31,32]

$$\Delta S_M(T, H) = S_M(T, H) - S_M(T, 0)$$

$$= \int_0^{H^{\mathrm{max}}} \left[\frac{\partial M(T, H)}{\partial T} \right]_H dH, \qquad (1)$$

where H^{max} is the maximum of external magnetic field. Figures 4(a) and 4(b) plot the temperature-dependent ΔS_M $[\Delta S_M(T)]$ under different H with $H//ab$ and $H//c$, respectively. A peak at T_C occurs to each curve, which indicates the change of magnetic entropy reaches the maximum at T_C. However, the values of $\Delta S_M(T)$ with $H//ab$ under fixed field are smaller than those with $H//c$. Meanwhile, the parameters of $|\Delta S_M(T, H)|$ curves follow a series of power laws dependent on the field as [30,33]

$$\left|\Delta S_M^{\mathrm{max}}(T)\right| \propto H^n$$

$$P_{\Delta S} \propto H^c, \qquad (2)$$

where $|\Delta S_M^{\mathrm{max}}|$ is the maximum of the $|\Delta S_M(T)|$, and $P_{\Delta S}$ is relative cooling power, which is defined as $P_{\Delta S} = |\Delta S_M^{\mathrm{max}} \times \delta_{FWHM}|$ (δ_{FWHM} is the full width at half maximum). Figures 5(a) and 5(b) plot the field dependence of $|\Delta S_M^{\mathrm{max}}|$ with $H//ab$ and $H//c$ respectively, where the fitted curves give $n = 0.854(1)$ for $H//ab$ and $n = 0.695(6)$ for $H//c$. Figures 5(c) and 5(d) depict the field dependence of $P_{\Delta S}$ with $H//ab$ and $H//c$, where $c = 1.364(8)$ for $H//ab$ and $c = 1.172(2)$ for $H//c$.

Intrinsically, the exponents n and c are determined by the critical exponents as [34]

$$n = 1 + \frac{\beta - 1}{\beta + \gamma}$$

$$c = 1 + \frac{1}{\delta}, \qquad (3)$$

where β (associated to the spontaneous magnetization), γ (corresponding to the initial susceptibility), and δ (correlating to the critical magnetization) are critical exponents. In addition, these obtained critical exponents should fulfill the Widom scaling law [35]:
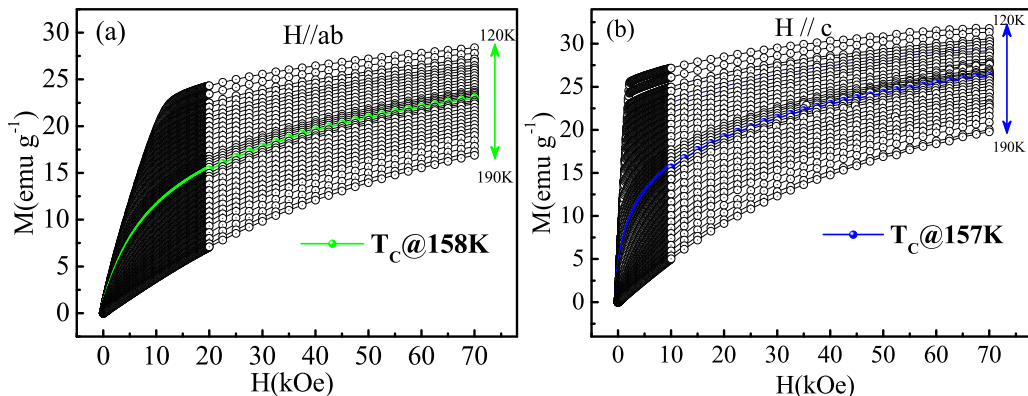
$$\delta = 1 + \frac{\gamma}{\beta}. \qquad (4)$$

FIG. 3. Field dependence of isothermal initial magnetization $[IM(H)]$ around T_C with (a) $H//ab$ and (b) $H//c$.
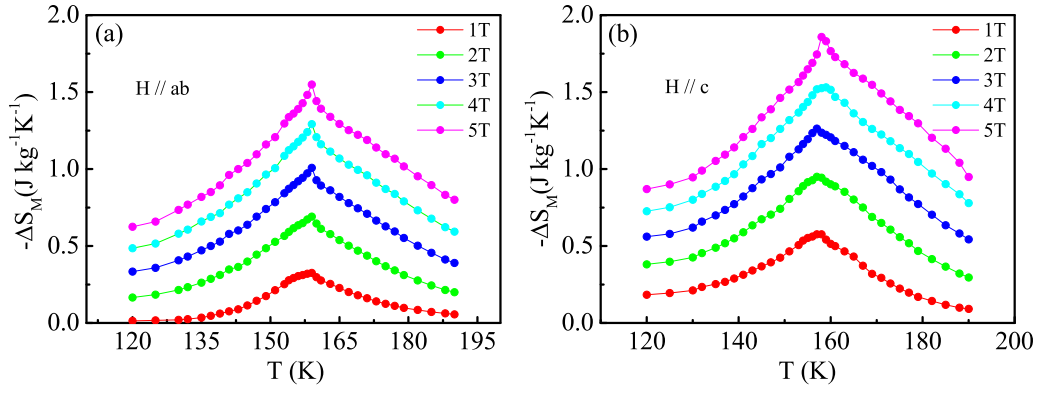
FIG. 4. Temperature dependence of magnetic entropy change [$\Delta S_M(T)$] under different fields with (a) $H//ab$ and (b) $H//c$.

Based on Eqs. (3) and (4), the critical exponents are obtained as $\beta = 0.714(3)$, $\gamma = 1.243(7)$, and $\delta = 2.741(1)$ for $H//ab$, while $\beta = 0.361(3)$, $\gamma = 1.736(7)$, and $\delta = 5.806(8)$ for $H//c$. This method based on the magnetic entropy change directly fits out the critical exponents, which avoids the deviation caused by the multistep nonlinear fitting in the previous conventional method [36–38].

Meanwhile, the critical exponent δ can be examined by the critical isothermal analysis at the critical temperature. Generally, T_C can be roughly determined from the minimum of the dM/dT curve. However, T_C is usually affected by the external field. Thus, more precisely, T_C should be determined

by the magnetic specific heat change [$\Delta C_P(T, H)$] [39]:

$$\Delta C_p(T, H) = C_p(T, H) - C_p(T, 0) = T\frac{\partial \Delta S_M(T, H)}{\partial T}. \quad (5)$$

The $\Delta C_P(T)$ curves under different H with $H//ab$ and $H//c$ are plotted in Figs. 6(a) and 6(b), respectively. With the decrease of temperature, ΔC_P changes from positive in the paramagnetic phase to negative in ferromagnetic one. At the critical point T_C, all $\Delta C_P(T)$ curves cross over the zero point. Thus, when $\Delta C_P = 0$, it is determined that $T_C = 158.5(2)$ K for $H//ab$ and $T_C = 157.2(2)$ K for $H//c$. The critical exponent δ can be obtained by the critical isothermal analysis of
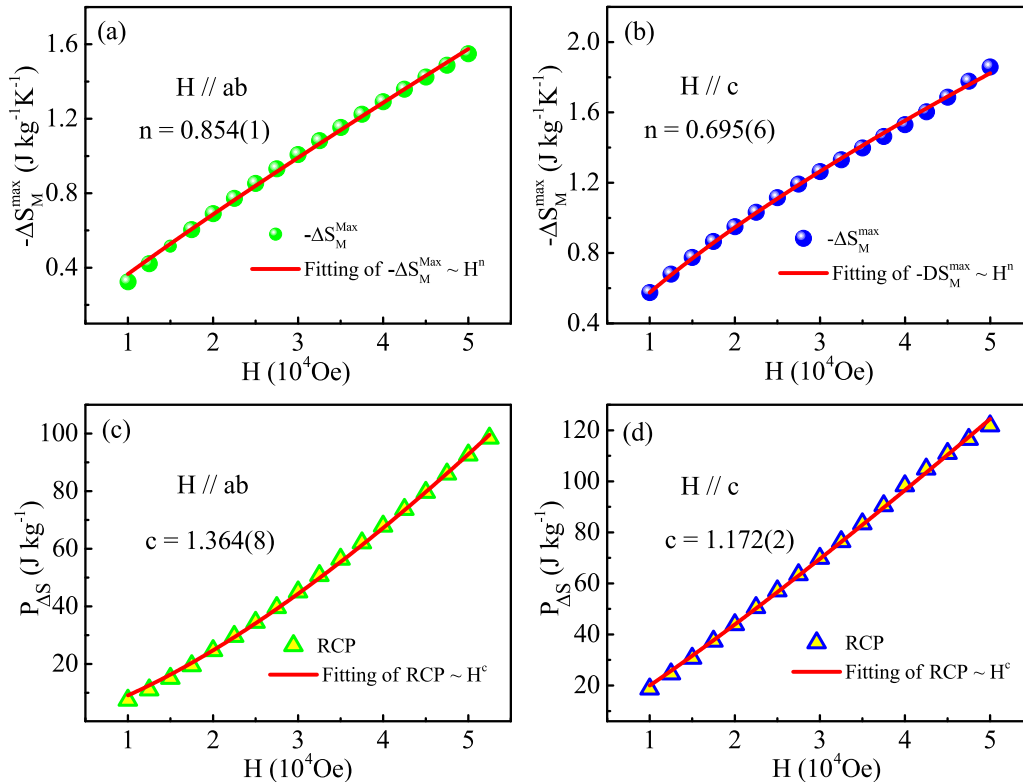

FIG. 5. Field-dependent parameters of $\Delta S_M(T)$: (a) $-\Delta S_M^{\text{max}}$ for $H//ab$ and (b) that for $H//c$; (c) $P_{\Delta S}$ for $H//ab$ and (d) that for $H//c$ (curves are fitted by power laws).
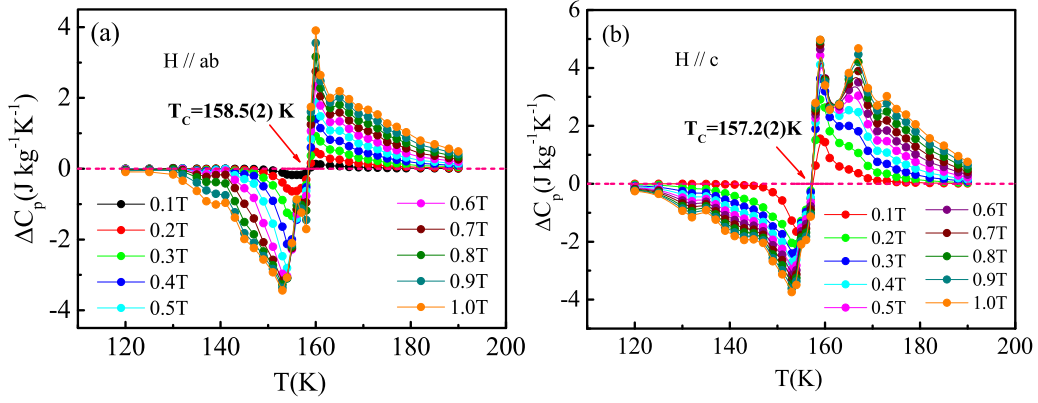
FIG. 6. Temperature dependence of magnetic specific heat $[C_P(T)]$ for (a) $H//ab$ and (b) for $H//c$.

the $IM(H)$ at the critical point. At T_C, there is [40]

$$M = DH^{1/\delta}, \quad \varepsilon = 0, \quad T = T_C, \quad (6)$$

where D is the critical amplitude and $\varepsilon = (T - T_C)/T_C$ is the reduced temperature. Consequently, the slope of $\log(M)$ versus $\log(H)$ yields $1/\delta$. Figure 7(a) gives the $IM(H)$ curve at $T_C = 158$ K for $H//ab$ and $T_C = 157$ K for $H//c$. It can be seen that these two curves magnetize along different paths, which imply different magnetizing behaviors. The fitting results by Eq. (6) are plotted on a log-log scale in Figs. 7(b) and 7(c) for $H//ab$ and $H//c$, respectively. Subsequently, $\delta = 2.883(4)$ is obtained for $H//ab$, which is close to the theoretical $\delta = 3.0$ of the mean-field model [41]. Meanwhile, $\delta = 4.590(7)$ is generated for $H//c$, which approaches $\delta = 4.8$ of the 3D Heisenberg model [41]. The δ values obtained by the critical isothermal analysis are in agreement with those yielded by the magnetic entropy changes. The self-consistency confirms the reliability of the obtained critical exponents.

The principal of universality is a guided law in the critical phenomenon of phase transition. According to the principal of universality, $\Delta S_M(T, H)$ can be scaled into a universal
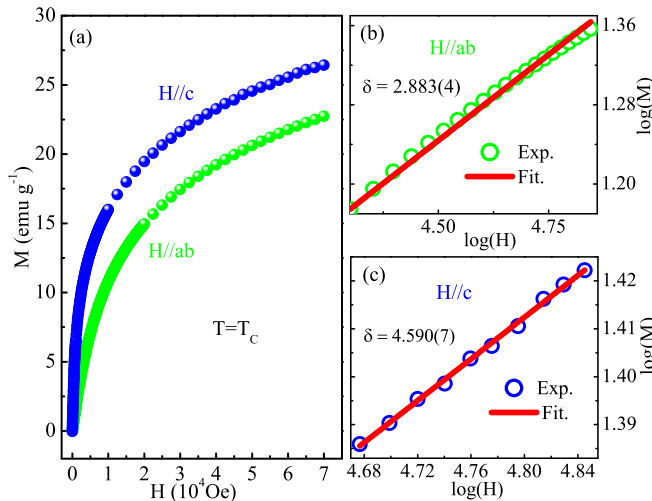

FIG. 7. (a) Initial isothermal magnetization at T_C for $H//ab$ and $H//c$; [(b), (c)] critical isothermal analysis for $IM(H)$ at T_C for $H//ab$ and $H//c$ respectively (lines are fitted).

curve independent of the external field [30]. The magnetic entropy change can be normalized as $\Delta S'_M = \Delta S_M / \Delta S_M^{\max}$. The temperature is normalized into a rescaled temperature θ defined as [34]

$$\theta = \begin{cases} \theta_- = (T_C - T)/(T_{r1} - T_C), & T \leqslant T_C \\ \theta_+ = (T - T_C)/(T_{r2} - T_C), & T > T_C \end{cases}, \quad (7)$$

where T_{r1} and T_{r2} are the reference temperatures below and above T_C respectively. Here, T_{r1} and T_{r2} are defined as $\Delta S_M(T_{r1}, T_{r2}) = \frac{1}{2}\Delta S_M^{\max}$. In other words, T_{r1} and T_{r2} just correspond to $\theta = -1$ and $\theta = +1$ after normalization. The normalized $\Delta S'_M(\theta)$ curves with $H//ab$ and $H//c$ are shown in Figs. 8(a) and 8(b) respectively. All curves under different H collapse into a single universal curve, which are independent of the external field. The good scaling and convergence of $\Delta S_M(T, H)$ curves indicate that the magnetic phase transition of $Fe_{3-x}GeTe_2$ is of a second-order type [42].

For a second-order magnetic transition, the $\Delta S_M(H)$ versus T curves should follow scaled equation of state $H/M^\delta = f(\varepsilon/M^{1/\beta})$, where the $\Delta S_M(T, H)$ can be rewritten in the form of [43,44]

$$\Delta S_M(T, H) = H^{\frac{1-\alpha}{\Delta}} g\left(\frac{\varepsilon}{H^{1/\Delta}}\right) \quad (8)$$

where critical exponents α and Δ can be obtained by Rush-brooke's law [40]:

$$\alpha = 2 - 2\beta - \gamma$$
$$\Delta = \delta\beta. \quad (9)$$

It is obtained that $\alpha = -0.672(3)$ and $\Delta = 2.059(6)$ for $H//ab$, while $\alpha = -0.459(3)$ and $\Delta = 1.658(6)$ for $H//c$. Figures 8(c) and 8(d) display $-\Delta S_M/H^{(1-\alpha)/\Delta}$ versus $\varepsilon/H^{1/\Delta}$ for $H//ab$ and $H//c$, respectively. All curves for $H//ab$ and $H//c$ collapse into two independent universal curves respectively in Figs. 8(c) and 8(d). The good scaling and collapse of the $\Delta S_M(T, H)$ curves confirm the reliability and validity of the obtained critical exponents.

The critical exponents of $Fe_{3-x}GeTe_2$ with $H//ab$ and $H//c$, as well as other related materials and theoretical models [28,29,37,38,41,45–47], are listed in Table I for comparison. As is known, the easy axis of magnetization of $Fe_{3-x}GeTe_2$ is along the c axis. Thus, previous studies are mainly focused on the magnetism under $H//c$. However, the critical behavior
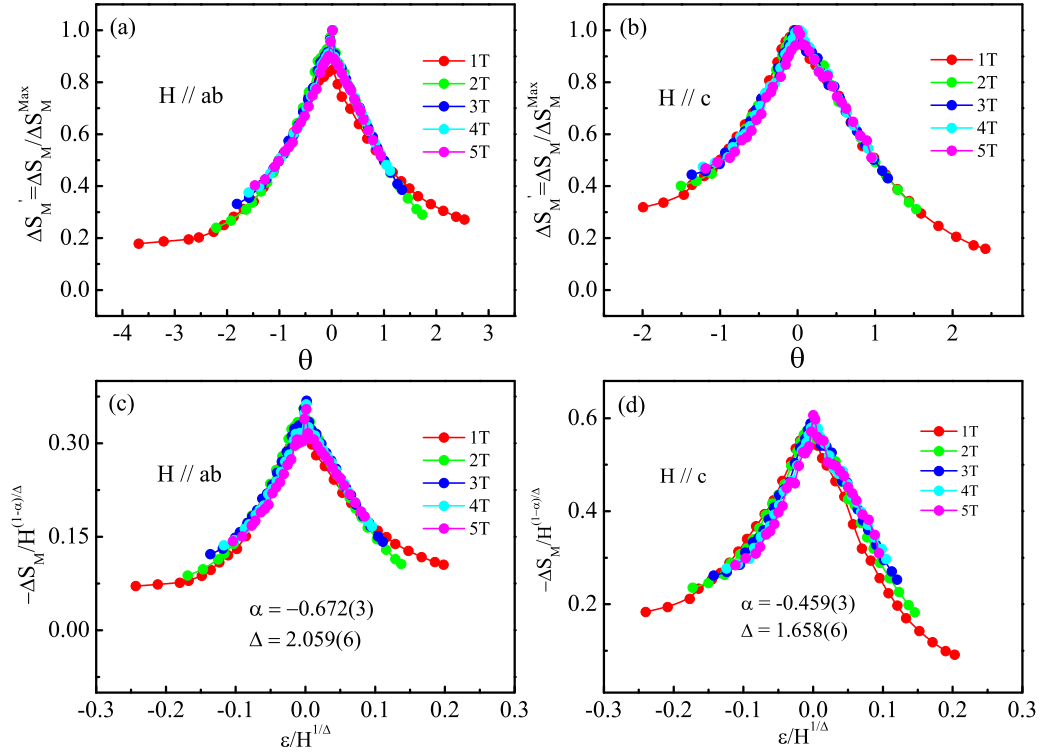
FIG. 8. Scaled $\Delta S_M(T, H)$ curves: normalized $\Delta S_M/\Delta S_M^{\max}$ vs θ for (a) $H//ab$ and for (b) $H//c$; $-\Delta S_M/H^{(1-\alpha)/\Delta}$ vs $\varepsilon/H^{1/\Delta}$ for (c) $H//ab$ and for (d) $H//c$.

under $H//ab$ has not been intensively studied. The critical exponents with $H//c$ have been obtained by Liu *et al.* as $\beta = 0.372(4)$, $\gamma = 1.265(1)$, and $\delta = 4.50(1)$ [28]. Their results with $H//c$ are close to the theoretical prediction of 3D-Heisenberg model [28]. In addition, it has demonstrated that the Fe vacancy has rare effect on the universality class of the critical behaviors [28,48]. Our results of critical exponents with $H//c$ are in agreement with previous reports, which confirms the reliability of this method and results. The 3D Heisenberg model generally indicates a short-range magnetic coupling. Thus, the critical exponents with $H//c$ imply that

the magnetic coupling with $H//c$ is of a short-range type in $Fe_{3-x}GeTe_2$.

On the other hand, the critical exponents with $H//ab$ are obtained as $\beta = 0.7143(3)$, $\gamma = 1.243(7)$, and $\delta = 2.883(4)$, which are different from those with $H//c$. It is noticed that the magnetizing behaviors around T_C are different between $H//ab$ and $H//c$, as shown in Figs. 3 and 7. From Table I, it can be seen that critical exponents with $H//ab$ belong to the universality class of the mean-field model, which indicates a long-range magnetic coupling. This result is also consistent with the Stoner model, which is suggested to describe the

TABLE I. Comparison of critical exponents of $Fe_{3-x}GeTe_2$ with different theoretical models and related materials (MEC, magnetic entropy change; KFm Kouvel-Fisher plot; MAP, modified Arrott plot).

Composition	Technique	Ref.	T_C (K)	β	γ	δ
$Fe_{3-x}GeTe_2^{H//ab}$	MEC	This work	158.5(2)	0.714(3)	1.243(7)	2.741(1)
$Fe_{3-x}GeTe_2^{H//c}$	MEC	This work	157.2(2)	0.361(3)	1.736(7)	5.806(8)
$Fe_{3-x}GeTe_2^{H//c}$	KF	[28]	151.25(5)	0.372(4)	1.265(1)	4.50(1)
$Cr_2Ge_2Te_6^{H//c}$	MEC	[29]	66.4	0.177(9)	1.746(8)	10.869(5)
$Cr_2Ge_2Te_6^{H//c}$	KF	[37]	67.9	0.240(6)	1.000(5)	5.032(5)
$Cr_2Ge_2Te_6^{H//c}$	MAP	[38]	62.7	0.196(3)	1.32(5)	7.73(1)
$CrI_3^{H//c}$	KF	[45]	60.3	0.260(4)	1.136(6)	5.37(4)
$CrI_3^{H//c}$	KF	[46]	60.5	0.323(6)	0.835(5)	3.585(6)
Mean-field	Theory	[41]		0.5	1.0	3.0
D-Heisenberg	Theory	[41]		0.365	1.386	4.8
D-Ising	Theory	[41]		0.325	1.24	4.82
D-XY	Theory	[41]		0.346	1.316	4.81
Tricritical mean-field	Theory	[47]		0.25	1.0	5.0

itinerant ferromagnetism in this system [6,23]. Moreover, the generalized Rhodes-Wohlfarth ratio also suggests an itinerant magnetism in this system [25]. The different critical behaviors between $H//ab$ and $H//c$ imply that the types of magnetic coupling in $Fe_{3-x}GeTe_2$ are influenced by the external magnetic field, especially around T_C. It is known that the magnetic fluctuation is usually very strong near the phase transition temperature [49]. Therefore, the magnetic correlation around T_C can be easily influenced by the external disturbances such as magnetic field, pressure, optics, *etc*. When the external field is applied along different directions, the magnetic coupling evolves into different types. Therefore, in $Fe_{3-x}GeTe_2$, the field-dependent critical exponents stem from the field-dependent magnetic coupling. In fact, the field-dependent anisotropic magnetic entropy changes and magnetic behaviors have also been observed in $Cr_2Ge_2Te_6$ [24], which indicates that this field-dependent magnetic coupling may commonly exist in these systems.

IV. CONCLUSIONS

In summary, the anisotropic magnetization, magnetic entropy change, and critical behaviors of the itinerant ferromagnetic $Fe_{3-x}GeTe_2$ ($x \approx 0.28$) are investigated. The $M(\varphi)$ curves show that the easy magnetic axis is along the c axis,

while it exhibits absolute isotropic characteristics in the ab plane. The $\Delta S_M(T, H)$ curves show anisotropic features when the external magnetic field applied along the c axis ($H//c$) and ab plane ($H//ab$), respectively. The fitting of field-dependent parameters of ΔS_M gives the critical exponents $\beta = 0.361(3)$, $\gamma = 1.736(7)$, and $\delta = 5.806(8)$ for $H//c$, while $\beta = 0.714(3)$, $\gamma = 1.243(7)$, and $\delta = 2.741(1)$ for $H//ab$. The critical exponents with $H//c$, in agreement with the previous reports belong to the theoretical prediction of 3D Heisenberg model, which suggests a short-range magnetic coupling. However, the critical exponents with $H//c$ are close to those of mean-field model, which indicates a long-range magnetic coupling. The anisotropic critical exponents suggest that the magnetic coupling in $Fe_{3-x}GeTe_2$ is dependent on orientations of applied magnetic field.

[1] B. Huang, G. Clark, E. Navarro-Moratalla, D. Klein, R. Cheng, K. Seyler, D. Zhong, E. Schmidgall, M. McGuire, D. Cobden, W. Yao, D. Xiao, P. Jarillo-Herrero, and X. Xu, Nature (London) **546**, 270 (2017).

[2] D. Klein, D. MacNeill, J. Lado, D. Soriano, E. Navarro-Moratalla, K. Watanabe, T. Taniguchi, S. Manni, P. Canfield, J. Fernández-Rossier, and P. Jarillo-Herrero, Science **360**, 1218 (2018).

[3] M. Gibertini, M. Koperski, A. Morpurgo, and K. Novoselov, Nat. Nanotech. **14**, 408 (2019).

[4] T. Song, X. Cai, M. Tu, X. Zhang, B. Huang, N. Wilson, K. Seyler, L. Zhu, T. Taniguchi, K. Watanabe, M. McGuire, D. Cobden, D. Xiao, W. Yao, and X. Xu, Science **360**, 1214 (2018).

[5] C. Gong, L. Li, Z. Li, H. Ji, A. Stern, Y. Xia, T. Cao, W. Bao, C. Wang, Y. Wang, Z. Qiu, R. Cava, S. Louie, J. Xia, and X. Zhang, Nature (London) **546**, 265 (2017).

[6] Y. Deng, Y. Yu, Y. Song, J. Zhang, N. Wang, Z. Sun, Y. Yi, Y. Wu, S. Wu, J. Zhu, J. Wang, X. Chen, and Y. Zhang, Nature (London) **563**, 94 (2018).

[7] B. Huang, G. Clark, D. Klein, D. MacNeill, E. Navarro-Moratalla, K. Seyler, N. Wilson, M. McGuire, D. Cobden, D. Xiao, W. Yao, P. Jarillo-Herrero, and X. Xu, Nat. Nanotech. **13**, 544 (2018).

[8] Z. Wang, T. Zhang, M. Ding, B. Dong, Y. Li, M. Chen, X. Li, J. Huang, H. Wang, X. Zhao, Y. Li, D. Li, C. Jia, L. Sun, H. Guo, Y. Ye, D. Sun, Y. Chen, T. Yang, J. Zhang, S. Ono, Z. Han, and Z. Zhang, Nat. Nanotech. **13**, 554 (2018).

[9] S. Chong, K. Han, A. Nagaoka, R. Tsuchikawa, R. Liu, H. Liu, Z. Vardeny, D. Pesin, C. Lee, T. Sparks, and V. Deshpande, Nano Lett. **18**, 8047 (2018).

[10] K. Kim, J. Seo, E. Lee, K. Ko, B. Kim, B. Jang, J. Ok, J. Lee, Y. Jo, W. Kang, J. Shim, C. Kim, H. Yeom, B. Min, B. Yang, and J. Kim, Nat. Mater. **17**, 794 (2018).

[11] Y. Wang, C. Xian, J. Wang, B. Liu, L. Ling, L. Zhang, L. Cao, Z. Qu, and Y. Xiong, Phys. Rev. B **96**, 134428 (2017).

[12] Y. Liu, E. Stavitski, K. Attenkofer, and C. Petrovic, Phys. Rev. B **97**, 165415 (2018).

[13] C. Tan, J. Lee, S. Jung, T. Park, S. Albarakati, J. Partridge, M. Field, D. McCulloch, L. Wang, and C. Lee, Nat. Commun. **9**, 1554 (2018).

[14] Y. Zhang, H. Lu, X. Zhu, S. Tan, W. Feng, Q. Liu, W. Zhang, Q. Chen, Y. Liu, X. Luo, D. Xie, L. Luo, Z. Zhang, and X. Lai, Sci. Adv. **4**, eaao6791 (2018).

[15] J.-X. Zhu, M. Janoschek, D. S. Chaves, J. C. Cezar, T. Durakiewicz, F. Ronning, Y. Sassa, M. Mansson, B. L. Scott, N. Wakeham, E. D. Bauer, and J. D. Thompson, Phys. Rev. B **93**, 144404 (2016).

[16] G. D. Nguyen, J. Lee, T. Berlijn, Q. Zou, S. M. Hus, J. Park, Z. Gai, C. Lee, and A.-P. Li, Phys. Rev. B **97**, 014425 (2018).

[17] N. Leon-Brito, E. Bauer, F. Ronning, J. Thompson, and R. Movshovich, J. Appl. Phys. **120**, 083903 (2016).

[18] H. Deiseroth, K. Aleksandrov, C. Reiner, L. Kienle, and R. Kremer, Eur. J. Inorg. Chem. **2006**, 1561 (2006).

[19] A. F. May, S. Calder, C. Cantoni, H. Cao, and M. A. McGuire, Phys. Rev. B **93**, 014411 (2016).

[20] Q. Li, M. Yang, C. Gong, R. Chopdekar, A. N'Diaye, J. Turner, G. Chen, A. Scholl, P. Shafer, E. Arenholz, A. Schmid, S. Wang, K. Liu, N. Gao, A. Admasu, S. Cheong, C. Hwang, J. Li, F. Wang, X. Zhang, and Z. Qiu, Nano Lett. **18**, 5974 (2018).

[21] Z. Wang, D. Sapkota, T. Taniguchi, K. Watanabe, D. Mandrus, and A. Morpurgo, Nano. Lett. **18**, 4303 (2018).

[22] S. Calder, A. I. Kolesnikov, and A. F. May, Phys. Rev. B **99**, 094423 (2019).

[23] H. L. Zhuang, P. R. C. Kent, and R. G. Hennig, Phys. Rev. B **93**, 134407 (2016).

[24] Y. Liu and C. Petrovic, Phys. Rev. Mater. **3**, 014001 (2019).

[25] B. Chen, J. H. Yang, H. D. Wang, M. Imai, H. Ohta, C. Michioka, K. Yoshimura, and M. H. Fang, J. Phys. Soc. Jpn. **82**, 124711 (2013).

[26] V. Verchenko, A. Tsirlin, A. Sobolev, I. Presniakov, and A. Shevelkov, Inorg. Chem. **54**, 8598 (2015).

[27] J. Yi, H. Zhuang, Q. Zou, Z. Wu, G. Cao, S. Tang, S. Calder, P. Kent, D. Mandrus, and Z. Gai, 2D Mater. **4**, 011005 (2017).

[28] Y. Liu, V. N. Ivanovski, and C. Petrovic, Phys. Rev. B **96**, 144429 (2017).

[29] W. Liu, Y. Dai, Y.-E. Yang, J. Fan, L. Pi, L. Zhang, and Y. Zhang, Phys. Rev. B **98**, 214420 (2019).

[30] V. Franco, J. Blazquez, and A. Conde, Appl. Phys. Lett. **89**, 222512 (2006).

[31] V. Pecharsky and K. Gscheidner, J. Magn. Magn. Mater. **200**, 44 (1999).

[32] D. Griffiths, *Introduction to Electrodynamics*, 3rd ed. (Prentice Hall, Englewood Cliffs, NJ, 1999), pp. 559–562.

[33] V. Franco, A. Conde, J. Romero-Enrique, and J. Blazquez, J. Phys.: Condens. Matter **20**, 285207 (2008).

[34] V. Franco and A. Conde, Int. J. Refrigerat. **33**, 465 (2010).

[35] L. P. Kadanoff, Physics(Long Island City, N.Y.) **2**, 263 (1966).

[36] J. Fan, L. Ling, B. Hong, L. Zhang, L. Pi, and Y. Zhang, Phys. Rev. B **81**, 144426 (2010).

[37] G. T. Lin, H. L. Zhuang, X. Luo, B. J. Liu, F. C. Chen, J. Yan, Y. Sun, J. Zhou, W. J. Lu, P. Tong, Z. G. Sheng, Z. Qu, W. H. Song, X. B. Zhu, and Y. P. Sun, Phys. Rev. B **95**, 245212 (2017).

[38] Y. Liu and C. Petrovic, Phys. Rev. B **96**, 054406 (2017).

[39] X. Zhang, G. Wen, F. Wang, W. Wang, C. Yu, and G. Wu, Appl. Phys. Lett. **77**, 3072 (2000).

[40] H. E. Stanley, *Introduction to Phase Transitions and Critical Phenomena* (Oxford University Press, London, 1971).

[41] S. N. Kaul, J. Magn. Magn. Mater. **53**, 5 (1985).

[42] C. Romero-Muniz, R. Tamura, S. Tanaka, and V. Franco, Phys. Rev. B **94**, 134401 (2016).

[43] B. Widom, J. Chem. Phys. **43**, 3898 (1965).

[44] R. Griffiths, Phys. Rev. Lett. **423**, 17 (1969).

[45] Y. Liu and C. Petrovic, Phys. Rev. B **97**, 014420 (2018).

[46] G. Lin, X. Luo, F. Chen, J. Yan, J. Gao, Y. Sun, W. Tong, P. Tong, W. Lu, Z. Sheng, W. Song, X. Zhu, and Y. Sun, Appl. Phys. Lett. **112**, 072405 (2018).

[47] K. Huang, *Statistical Mechanics*, 2nd ed. (Wiley, New York, 1987).

[48] B. Liu, Y. Zou, S. Zhou, L. Zhang, Z. Wang, H. Li, Z. Qu, and Y. Zhang, Sci. Rep. **7**, 6184 (2016).

[49] H. Wilhelm, M. Baenitz, M. Schmidt, U. K. Rößler, A. Leonov, and A. N. Bogdanov, Phys. Rev. Lett. **107**, 127203 (2011).